Nuclear Inst. and Methods in Physics Research, A 976 (2020) 164181

Contents lists available at ScienceDirect

Nuclear Inst. and Methods in Physics Research, A

journal homepage: www.elsevier.com/locate/nima

A hybrid analytical–numerical method for full energy peak efficiency calibration of a NaI detector

W. El-Gammal [a], K.M. El-Kourghly [a,*], M.S. El-Tahawy [a], M. Abdelati [a], A. Abdelsalam [b], W. Osman [b]

[a] Nuclear Safeguards and Physical Protection Department, Egyptian Nuclear and Radiological Regulatory Authority (ENRRA), Cairo, Egypt
[b] Physics department, faculty of science, Cairo University, Giza, Egypt

ARTICLE INFO

Keywords:
Analytical–numerical
Monte Carlo
Peak efficiency
Total efficiency
Peak-to-total ratio

ABSTRACT

A hybrid analytical–numerical method is proposed to determine the Full Energy Peak Efficiency (FEPE) of a NaI bare crystal for a point γ-source in the energy range 48–2040 keV. The efficiency is calculated at all possible source locations with respect to the detector and at a maximum Source-to-Detector (S–D) distance of 50 cm. The method combines an analytical formula used for total efficiency calculation with numerically calculated Peak-to-Total (P/T) ratios. The FEPE efficiencies are calculated by integrating the combined analytical formula. A computer code is written using the C programming language to solve the integration using Simpson's rule. The calculated values of the FEPE are found to be in agreement with these calculated using the Monte Carlo (MC) method with a maximum relative difference of about 2.5%. The main advantage of the proposed method is the extremely reduced runtime of calculation in comparison with the MC method.

1. Introduction

The peak efficiency or the FEPE of a radiation detector could be defined as the product of the photon interaction probability (total efficiency) and the likelihood that the interacting photon will be completely absorbed within the detector active-volume (P/T ratio). Peak efficiency is usually obtained using either relative or absolute methods. While relative methods usually provide accurate peak efficiency calibration curves, absolute methods could be considered whenever calibration standards are not available. In such cases, radiation transport codes, e.g., the general Monte Carlo N-Particle Code (MCNP), are used to calibrate radiation detectors mathematically.

Heath et al. [1,2] introduced a theoretical calculation of total efficiency in conjunction with an experimental determination of the P/T ratio. Unfortunately, the calibration curve of the P/T ratio generally requires single-energy γ-emitters. Most of these radio-nuclides are short-lived and therefore need to be regularly replaced. Moreover, the presence of low energy γ-rays and X-rays in most decay schemes makes the empirical determination of P/T ratios more complex.

Moens et al. [3] introduced the efficiency transfer method, which combines analytical formulas of the effective solid angle with experimentally measured peak efficiency for point sources. Many authors, e.g., Moens and Hoste [4], Mihaljević et al. [5], Wang et al. [6,7], Jiang et al. [8] applied Moen's method to calculate the FEPE of cylindrical detectors for different source configurations including point, disk, cylindrical and Marinelli-beaker.

Aguiar et al. [9] proposed a semi-empirical method to obtain the FEPE of a HPGe detector for co-axial [9] and perpendicular [10] positions of cylindrical sources by applying corrections to point-source measurements. Stanga et al. [11] developed a semi-empirical model for the FEPE calculation of HPGe detectors, including corrections for gamma attenuation. They considered the cases of point and cylindrical sources. Their method was based on an approximating mathematical model representing the detector as a virtual point. However, it involves some approximations and simplifications, so the application is restricted to limited source–detector configurations.

In the above review, it is obvious that the provided methods are based on experimental measurements for which standard sources must be available or utilize MC calculations, which is time-consuming. In this work, a hybrid method is presented to calculate the FEPE of a bare NaI detector. The method is based on theoretical calculations; consequently, no calibration sources are required. Furthermore, MC calculations are performed once to calculate the P/T ratio, and no additional MC calculation is needed, which saves much time.

2. Methods description

The proposed hybrid method is achieved through two main steps: First, analytical formulas to determine the total efficiency of a NaI crystal are derived. In the second step, an MC code is used to calculate the P/T ratios for different γ-energies at different source positions with

* Corresponding author.
E-mail addresses: kamelelkourghlt287@icloud.com, eaea_nsncrc@yahoo.com (K.M. El-Kourghly).

https://doi.org/10.1016/j.nima.2020.164181
Received 2 February 2020; Received in revised form 20 May 2020; Accepted 23 May 2020
Available online 8 June 2020
0168-9002/

respect to the detector and combined with the analytical formulas. The peak efficiency is then calculated by integrating the final analytical formula using Simpson's rule. A computer code is written using a C programming language to solve the integration.

2.1. Analytical calculations

The FEPE ϵ_p for a NaI detector is expressed as

$$\epsilon_p = \epsilon_t p/t, \tag{1}$$

where, ϵ_t is the total efficiency, that can be written as

$$\epsilon_t = \frac{\Omega}{4\pi} f_{abs.} f_t f_s, \tag{2}$$

where, $\frac{\Omega}{4\pi}$: is the fractional solid angle of the source subtended by the detector,

$f_{abs.} = 1 - e^{-\mu d_i}$: is the interaction (absorption) probability along the photon track d_i inside the detector material,

$f_t = e^{-\mu_i t_i}$ is the transmission probability through absorber i of thickness t_i and μ_i is the total linear attenuation coefficient and

f_s is the self-attenuation factor due to the source material.

For the form point-like sources and bare crystal, the factors f_s and f_t are equals to unity, therefore Eq. (2) is reduced to the form:

$$\epsilon_t = \frac{\Omega}{4\pi} f_{abs.}. \tag{3}$$

The Solid angle of the source subtended by the detector Ω is defined as

$$\Omega = \int_\theta \int_\phi d\theta d\phi \ \sin\theta, \tag{4}$$

where, θ (0–π) and ϕ (0–2π) are the polar and azimuthal angles respectively, knowing that the track length inside the detector of the γ-ray emitted from a specific location depends on its direction of incidence (i.e., angles θ and ϕ), thus the total efficiency can be given as

$$\epsilon_t = \frac{1}{4\pi} \int_0^{2\pi} \int_0^{\pi} d\theta d\phi \ (1 - e^{-\mu . d_i(\theta,\phi)}) \ \sin\theta, \tag{5}$$

Fig. 1 shows the possible γ-ray track inside detector body includes penetrating the upper surface of the detector and emerging from the bottom surface (case 1) or lateral surface (case 2), penetration of lateral surface and emerging from the bottom surface (case 3) or lateral surface again (case 4). Cases 3 and 4 could also be considered for the case where the source is located in the plane containing the upper surface of the detector or in between the planes containing the upper and lower sides of the detector.

Fig. 2(a)–(g) illustrates the all possible configurations representing the position of the source with respect to the detector in three-dimensional geometry. The different parameters used to determine the γ-ray track length are shown in figures with their boundary conditions (angles limitations) for each position. The parameters include the shift (ρ), perpendicular distance between source position and plane containing the upper detector surface (h), polar (θ_i), and azimuthal ϕ_i angles for each configuration.

Therefore, the analytical equation that could be used to calculate the total efficiency of the detector for any configuration can be written as follows

$$\epsilon_t = \frac{1}{2\pi} \sum_{n_i}^{n_m} \int_{\phi_n(1)}^{\phi_n(2)} \int_{\theta_{n,i}(1)}^{\theta_{n,m}(2)} d\theta d\phi \ (1 - e^{-\mu d_{n,i}}) \ \sin\theta, \tag{6}$$

where, n: is the configuration number, $n = 1, 2, 3, \ldots, 7$,

i: represents the number of terms of integration for the configuration number n, $i = 1, 2, 3, \ldots, m$ term and

$d_{n,i}$: is the possible path length of configuration number n and integration term number i.

All possible photon path lengths $d_{n,i}$ and polar angles are given in Appendix.

For the first two configurations azimuthal angle ϕ ranges from 0–π. For the third configuration the range become 0–$\frac{\pi}{2}$, while for the rest configurations the angle ranges from 0–$\sin^{-1}(\frac{R}{\rho})$.

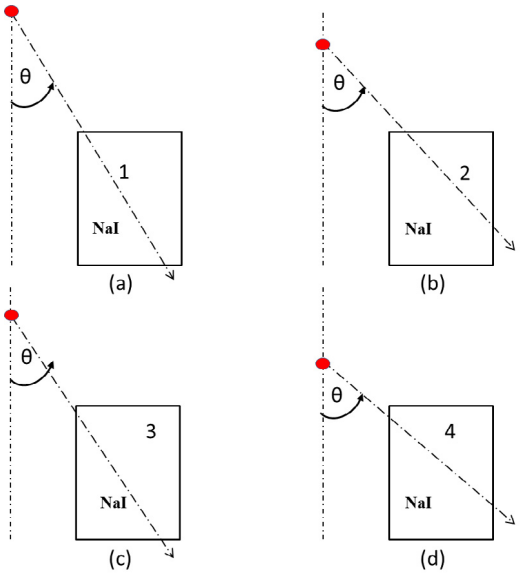

Fig. 1. The four possible path-lengths of photons through NaI detector.

Table 1
Possible double side penetration track $\rho \in [0, 50]$, $h \in [detector - base, L] \cup [5, 50]$.

	ρ	h (cm)
P1	0	
P2	[0, R)	≥5
P3	R	
P4		
P5		
P6	$>R$	0
P7		<0

2.2. MC simulation

The NaI bare crystal ($3^{in} \times 3^{in}$) is modeled using the MCNPX code [12] which contains F8 tally. The pulse height tally is used to calculate the efficiency of the detector. The peak efficiencies are calculated, assuming that the point source is located at different positions (configurations) with respect to the detector, as illustrated in Fig. 3 and explained in Table 1. The positions include, the co-axial position P1, shifted positions at a distance ρ less than the detector radius (R) of the detector (P2), above the detector edge (P3), greater than detector radius (P4), parallel (P6) and below the plane containing layer surface of the detector (P7).

The MC model is used to calculate both the total and peak efficiencies in the γ-energy range 48–2040 keV at the different configurations (P1-P7) and for S–D distances range 5–50 cm. The calculations were performed on a 2.66 GHz processor with a number of histories of 10^7 for all input files.

The selected γ-energy range encompasses all the possible interaction phenomena (photoelectric, Compton scattering and pair production processes).

A total of eleven γ-energies are considered for each configuration at a given distance.

To practically check the accuracy of the used method for P/T ratio calculation, it is important to compare the calculated values with experimental results. However, normally, experimental data are available for real detectors (not bare ones). Consequently, in addition to the bare detector modeled in this work, additional complete detector modeling is also considered only for checking with experimental data.

The obtained total and FEPE were used to calculate the P/T ratios at all distances and for each position by dividing the peak efficiency of the selected γ-energy line by the sum of efficiencies in all the energy

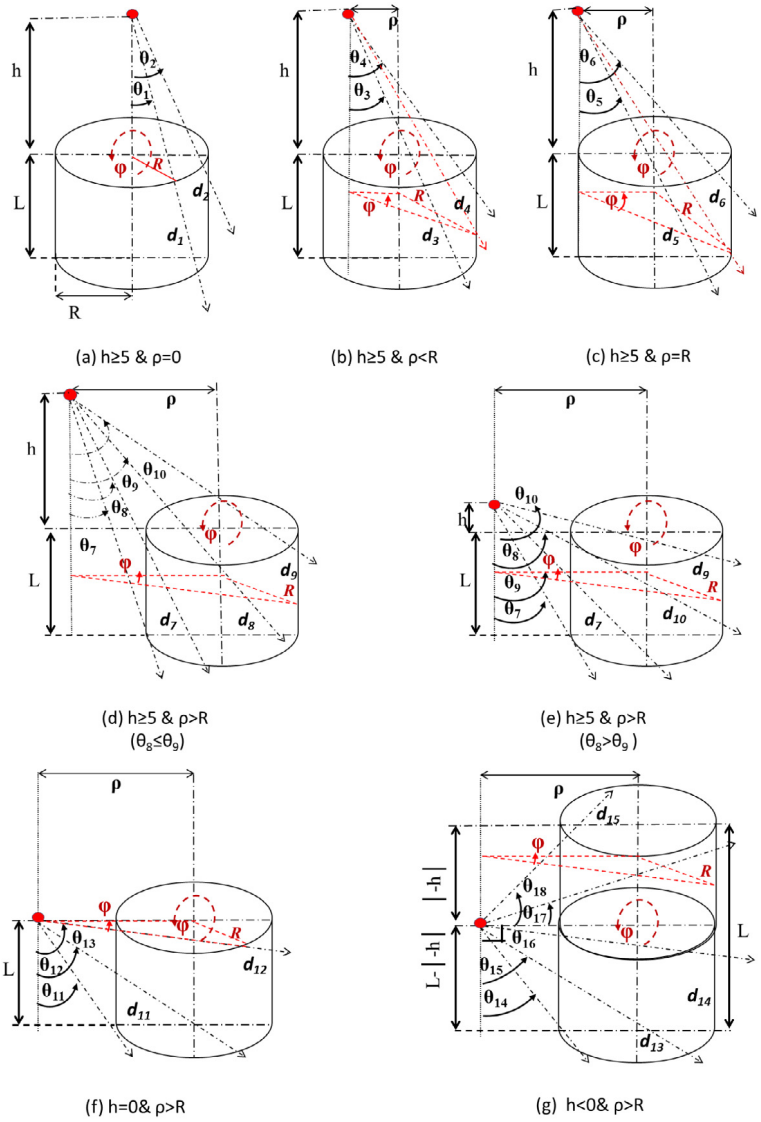

Fig. 2. Different S–D configurations with all possible locations and angles of integrals.

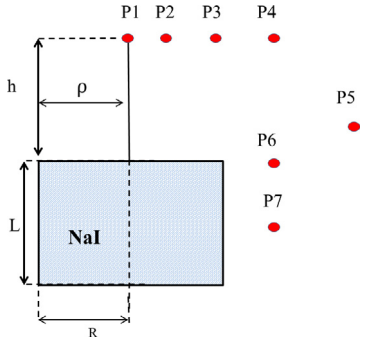

Fig. 3. S–D configurations for P/T determination.

bins above 1 keV. Due to the relatively small variation in the calculated P/T ratio with distance for each configuration, the P/T ratio for each configuration is obtained by averaging the P/T ratio results at different S–D distances from 5–50 cm, as given by the following equation

$$(P/T)_c = \frac{1}{n_d}\sum_{n_d}(p/t)_d, \tag{7}$$

where, $(P/T)_c$ is the P/T ratio for a given configuration c, $(p/t)_d$ is the P/T ratio at a distance d and n_d is the number of S–D distances at which P/T ratio is calculated for that configuration.

2.3. Numerical calculation

The FEPE in the energy range 48–2040 keV are calculated by multiplying the total efficiency Eq. (6) by the calculated P/T ratios and use of Simpson's rule to solve the integration numerically with the aid of computer code, written using the C programming language. Calculation processes are carried out by dividing the integration limits for each of polar θ and azimuthal ϕ angles into 1000 intervals. The flowchart of the designed code used to solve the integration is illustrated in Fig. 4.

3. Results and discussion

In this work, the FEPE efficiency has been calculated for a point source at different γ-energy lines, located at arbitrary positions with respect to a NaI detector using a hybrid analytical–numerical method.

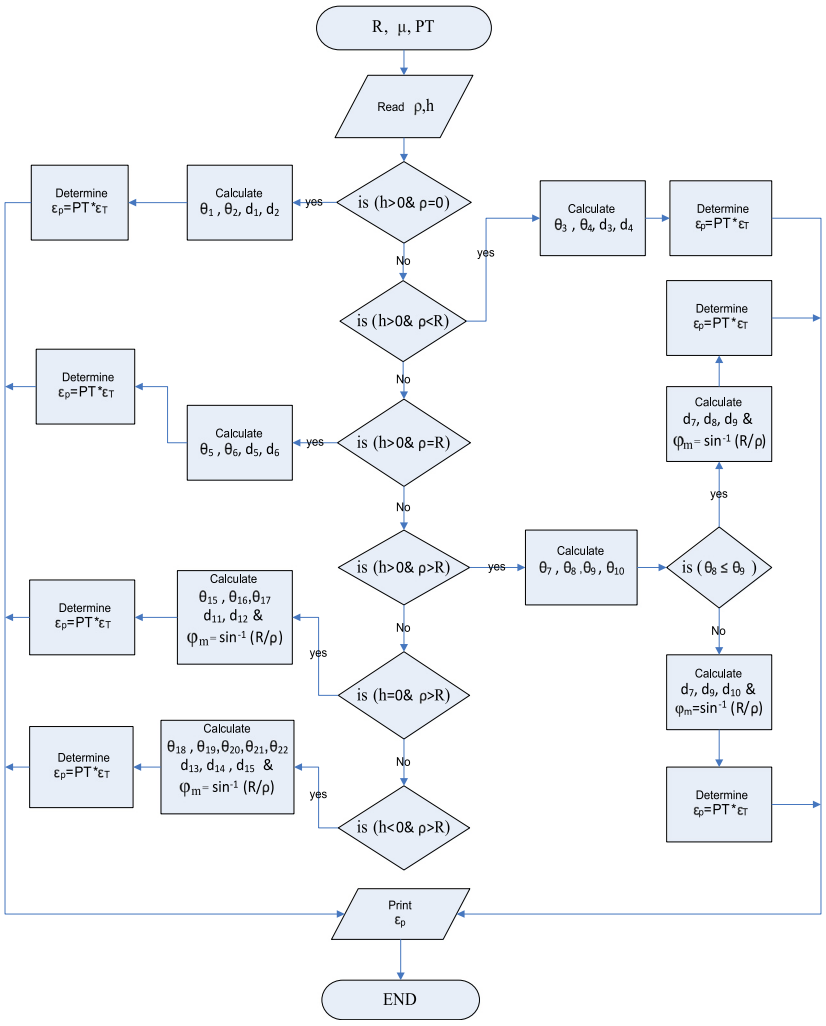

Fig. 4. Flow chart of the developed program.

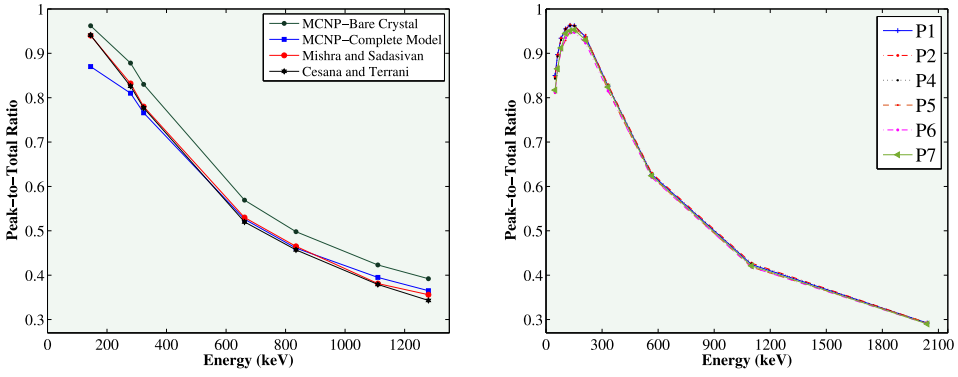

Fig. 5. P/T ratios vs. γ-energy lines for (a)Comparison of MCNP calculated and published P/T ratios data(b) Calculated using MCNP at different S–D configurations.

3.1. Peak-to-total ratio

Before calculating P/T ratios used in FEPE calculation, the accuracy of the used method had to be checked, as mentioned in Section 2.2. For this purpose, the complete model of the detector is created that simulates experimental work done by Mishra and Sadasivan [13]; and also simulates the theoretical work done by Cesana and Terrani [14]. The simulation is done for the NaI crystal ($3^{in}\times3^{in}$), while the source is located in a co-axial position distant 10 cm from the detector surface.

Fig. 5(a) illustrates the results of a simulation for bare, and complete modeled detector; and experimental and theoretical data. It is clear from the figure that the complete modeling of the detector gives results that are in agreement with experimental and theoretical values with a maximum relative difference of about 3.5% and 6%, respectively. For low energy, the P/T ratio deviates by 7% in comparison with Mishra

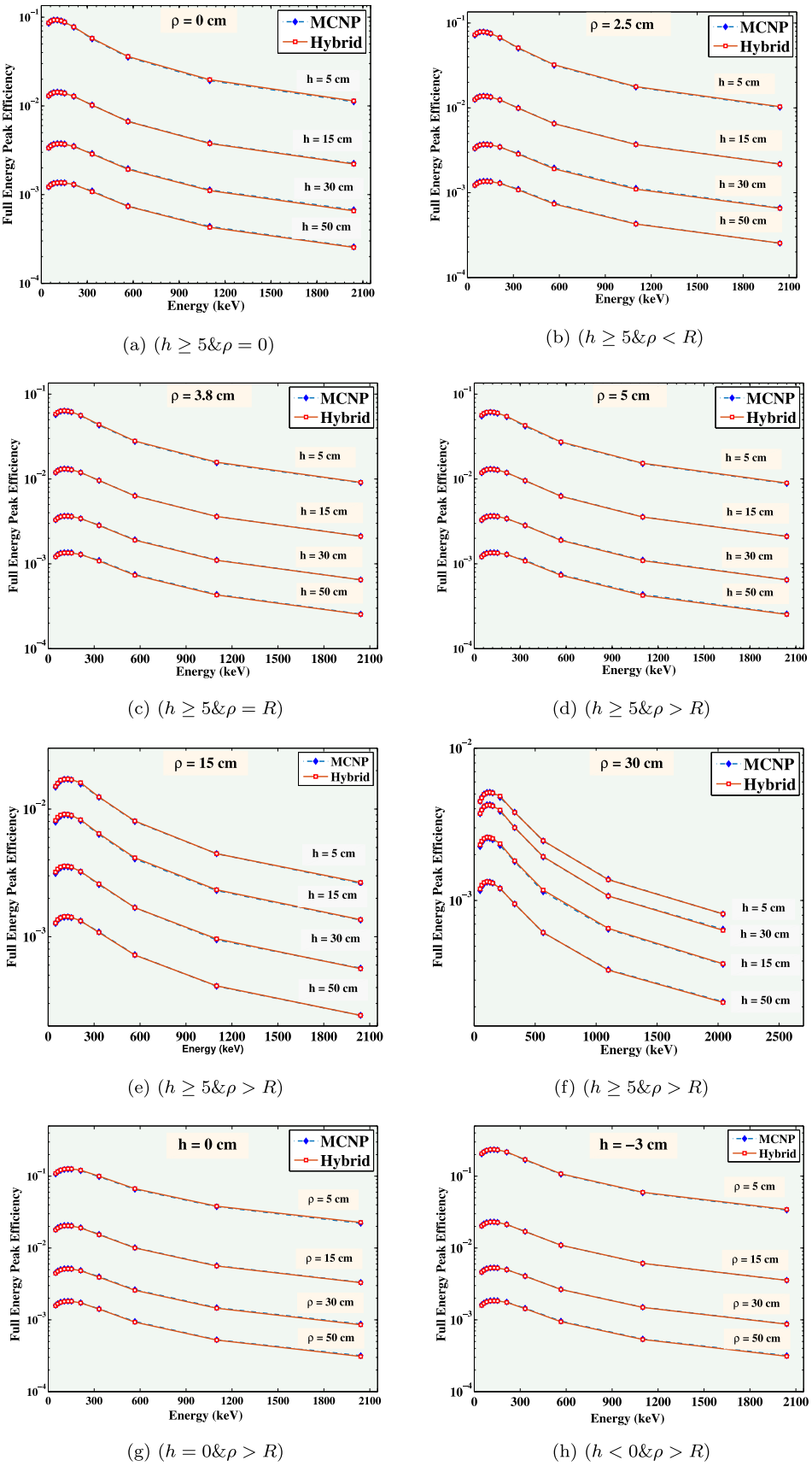

Fig. 6. Peak Efficiency vs. Energy comparison between MCNP and Hybrid for all the possible S–D configuration.

Table A.1
The possible photon path lengths and integration limits for polar angles.

No	Configuration	*Path Length*[a]		*Polar Angle*[b]		[a] *Path Length*
1	$(h \geq 5 \& \rho = 0)$	$d_{1,1}$	$d_1 = p_1$	$\theta_{1,1}(1)$	$\theta_0 = \theta_a$	$P_1 = l/\cos\theta$
				$\theta_{1,1}(2)$	$\theta_1 = \theta_b$	$P_2 = R/\sin\theta - d/\cos\theta$
		$d_{1,2}$	$d_2 = p_2$	$\theta_{1,1}(1)$		$P_3 = \rho^+/\sin\theta - h/\cos\theta$
				$\theta_{2,1}(1)$	$\theta_2 = \theta_c$	$P_4 = h + l/\cos\theta - \rho^-/\sin\theta$
2	$(h \geq 5 \& \rho < R)$	$d_{2,1}$	$d_3 = p_1$	$\theta_{2,1}(1)$	$\theta_0 = \theta_a$	$P_5 = \rho^+/\sin\theta$
				$\theta_{2,1}(2)$	$\theta_3 = \theta_d$	$P_6 = \rho^*/\sin\theta$
		$d_{2,2}$	$d_4 = p_3$	$\theta_{2,2}(1)$		$P_7 = l/\cos\theta - \rho^-/\sin\theta$
				$\theta_{2,2}(2)$	$\theta_4 = \theta_e$	$P_8 = l - h/\cos\theta - \rho^-/\sin\theta$
3	$(h \geq 5 \& \rho = R)$	$d_{3,1}$	$d_5 = p_1$	$\theta_{3,1}(1)$	$\theta_0 = \theta_a$	$P_8 = h/\cos\theta - \rho^-/\sin\theta$
				$\theta_{3,1}(2)$	$\theta_5 = \theta_d$	
		$d_{3,2}$	$d_6 = p_3$	$\theta_{3,2}(1)$		[b] *Polar Angles*
				$\theta_{3,2}(2)$	$\theta_6 = \theta_e$	
4	$(h \geq 5 \& \rho > R)$ $(\theta_8 \leq \theta_9)$	$d_{4,1}$	$d_7 = p_4$	$\theta_{4,1}(1)$	$\theta_7 = \theta_f$	
				$\theta_{4,1}(2)$	$\theta_8 = \theta_g$	$\theta_a = 0$
		$d_{4,2}$	$d_8 = p_1$	$\theta_{4,2}(1)$		$\theta_b = \tan^{-1}(R/h + l)$
				$\theta_{4,2}(2)$	$\theta_9 = \theta_d$	$\theta_c = \tan^{-1}(R/h)$
		$d_{4,3}$	$d_9 = p_5$	$\theta_{4,3}(1)$		$\theta_d = \tan^{-1}(\rho^+/h + l)$
				$\theta_{4,3}(2)$	$\theta_{10} = \theta_e$	$\theta_e = \tan^{-1}(\rho^+/h)$
5	$(h \geq 5 \& \rho > R)$ $(\theta_8 > \theta_9)$	$d_{5,1}$	$d_7 = p_4$	$\theta_{5,1}(1)$	$\theta_7 = \theta_f$	$\theta_f = \tan^{-1}(\rho^-/h + l)$
				$\theta_{5,1}(2)$	$\theta_9 = \theta_d$	$\theta_g = \tan^{-1}(\rho^-/h)$
		$d_{5,2}$	$d_9 = p_5$	$\theta_{5,2}(1)$		$\theta_h = \tan^{-1}(\rho^-/l)$
				$\theta_{5,2}(2)$	$\theta_8 = \theta_g$	$\theta_i = \tan^{-1}(\rho^+/l)$
		$d_{5,3}$	$d_{10} = p_6$	$\theta_{5,3}(1)$		$\theta_j = \tan^{-1}(\pi/2)$
				$\theta_{5,3}(2)$	$\theta_{10} = \theta_e$	$\theta_k = \tan^{-1}(\rho^-/l - \lvert h\rvert)$
6	$(h = 0 \& \rho > R)$	$d_{6,1}$	$d_{11} = p_7$	$\theta_{6,1}(1)$	$\theta_{11} = \theta_h$	$\theta_l = \tan^{-1}(\rho^+/l - \lvert h\rvert)$
				$\theta_{6,1}(2)$	$\theta_{12} = \theta_i$	$\theta_m = \tan^{-1}(\rho^-/\lvert h\rvert)$
		$d_{6,2}$	$d_{12} = p_6$	$\theta_{6,2}(1)$		$\theta_n = \tan^{-1}(\rho^+/\lvert h\rvert)$
				$\theta_{6,2}(2)$	$\theta_{13} = \theta_j$	
7	$(h < 0 \& \rho > R)$	$d_{7,1}$	$d_{13} = p_8$	$\theta_{7,1}(1)$	$\theta_{14} = \theta_k$	
				$\theta_{7,1}(2)$	$\theta_{15} = \theta_l$	
		$d_{7,2}$	$d_{14} = p_6$	$\theta_{7,2}(1)$		$\rho^+ = \rho\cos\phi + \sqrt{R^2 - \rho^2\sin^2\theta}$
				$\theta_{7,3}(1)$	$\theta_{16} = \theta_j$	
		$d_{6,3}$	$d_{15} = p_9$	$\theta_{7,3}(1)$	$\theta_{17} = \theta_m$	$\rho^- = \rho\cos\phi - \sqrt{R^2 - \rho^2\sin^2\theta}$
				$\theta_{7,3}(2)$	$\theta_{18} = \theta_n$	
		$d_{7,4}$	$d_{14} = p_6$	$\theta_{7,4}(1)$		$\rho^* = 2\times\sqrt{R^2 - \rho^2\sin^2\theta}$
				$\theta_{7,4}(2)$	$\theta_{16} = \theta_j$	

and Sadasivan [13], Cesana and Terrani [14], which may be attributed to the fact that the aluminum cover and crystal-to-cover distance are not well defined. Calculations indicated that an inaccuracy of 1 mm in aluminum cover causes an error of about 3% at 145 keV.

Based on the bare crystal model, the P/T ratios for different γ-energies are obtained for the different S–D configurations, as described in Section 2.2.

Fig. 5(b) shows the obtained values vs. γ-energy lines at the different source positions with respect to the detector. For each S–D configuration the calculated average P/T ratio over the considered distance 5–50 cm differs from that calculated at any specific distance by about 1% except for very low energies which may reach 3.5%.

3.2. Full energy peak efficiency

Using the proposed hybrid analytical–numerical method, the peak efficiencies of a bare NaI crystal are calculated for the different S–D configurations. The calculation time using the proposed method is always less than 1 s. The results were next compared to the corresponding calculated results based on MCNP. Fig. 6(a)–(h) presents a comparison between the proposed method and MC estimates of peak efficiencies against γ-energy lines for the considered S–D configurations described in Fig. 2.

The determined peak efficiencies using the proposed hybrid method were in agreement with MC calculations with a maximum relative difference of 2.5% for all possible S–D configurations. The estimated uncertainty on the data, concerning the MC calculations is always less than 1.5%.

4. Conclusion

In this work, a hybrid analytical–numerical method is introduced and checked to calculate the FEPE of a NaI detector due to the γ-ray point source. The method depends on the numerical integration of analytical formula, which combines an analytical equation for total efficiency calculation with P/T ratios obtained using MC calculations.

All possible S–D configurations are considered. The MC calculation to calculate the P/T ratios for each configuration is performed once, and the obtained values are directly substituted in the analytical formula. Consequently, no additional MC calculations are needed, which saves

much time when compared with pure MC calculations. In addition, the method does not depend on experimental measurements. The obtained results of the FEPE were found to be in agreement with MC with a maximum relative difference of 2.5%.

The work could be extended to include different sizes of NaI detectors. It could also be extended to include different forms of sources, including line, disk, and volume sources.

CRediT authorship contribution statement

W. El-Gammal: Conceptualization. **K.M. El-Kourghly:** Methodology, Software, Validation, Writing - original draft,. **M.S. El-Tahawy:** Supervision. **M. Abdelati:** Supervision. **A. Abdelsalam:** Supervision. **W. Osman:** Supervision.

Declaration of competing interest

The authors declare that they have no known competing financial interests or personal relationships that could have appeared to influence the work reported in this paper.

Appendix. The possible photon path lengths and integration limits for polar angles

See Table A.1.

References

[1] R.L. Heath, S.H. Vegors Jr., L.L. Marsden, Calculated efficiencies of cylindrical radiation detectors, Technical Report IDO-16370, Phillips Petroleum Co. Atomic Energy Div., Idaho Falls, Idaho, 1958.

[2] R.L. Heath, S.H. Vegors Jr., L.L. Marsden, Scintillation Spectrometry Gamma Ray Spectrum Catalogue, Technical Report IDO-16880-1, Phillips Petroleum Co. Atomic Energy Div., Idaho Falls, Idaho, 1964.

[3] L. Moens, J. De Donder, L. Xi-Lei, F. De Corte, A. De Wispelaere, A. Simonits, J. Hoste, Calculation of the absolute peak efficiency of gamma-ray detectors for different counting geometries, Nucl. Instrum. Methods Phys. Res. 187 (2–3) (1981) 451–472.

[4] L. Moens, J. Hoste, Calculation of the peak efficiency of high-purity germanium detectors, Int. J. Appl. Radiat. Isot. 34 (8) (1983) 1085–1095.

[5] N. Mihaljević, S. Jovanović, F. De Corte, B. Smodiš, R. Jaćimović, G. Medin, A. De Wispelaere, P. Vukotić, P. Stegnar, "EXTSANGLE"—An extension of the efficiency conversion program "SOLANG" to sources with a diameter larger than that of the Ge-detector, J. Radioanal. Nucl. Chem. 169 (1) (1993) 209–218.

[6] T.-K. Wang, W.-Y. Mar, T.-H. Ying, C.-H. Liao, C.-L. Tseng, HPGe detector absolute-peak-efficiency calibration by using the ESOLAN program, Appl. Radiat. Isot. 46 (9) (1995) 933–944.

[7] T.-K. Wang, W.-Y. Mar, T.-H. Ying, C.-L. Tseng, C.-H. Liao, M.-Y. Wang, HPGe detector efficiency calibration for extended cylinder and marinelli-beaker sources using the ESOLAN program, Appl. Radiat. Isot. 48 (1) (1997) 83–95.

[8] S. Jiang, J. Liang, J. Chou, U. Lin, W. Yeh, A hybrid method for calculating absolute peak efficiency of germanium detectors, Nucl. Instrum. Methods Phys. Res. A 413 (2–3) (1998) 281–292.

[9] J.C. Aguiar, E. Galiano, J. Fernandez, Peak efficiency calibration for attenuation corrected cylindrical sources in gamma ray spectrometry by the use of a point source, Appl. Radiat. Isot. 64 (12) (2006) 1643–1647.

[10] J.C. Aguiar, An analytical calculation of the peak efficiency for cylindrical sources perpendicular to the detector axis in gamma-ray spectrometry, Appl. Radiat. Isot. 66 (8) (2008) 1123–1127.

[11] D. Stanga, D. Radu, O. Sima, A new model calculation of the peak efficiency for HPGe detectors used in assays of radioactive waste drums, Appl. Radiat. Isot. 68 (7–8) (2010) 1418–1422.

[12] E. D.B. Pelowitz, MCNPX Users Manual Version 2.7.0" LA-CP-11-00438l, 2.7 ed., Los Alamos National Laboratory, 2011.

[13] U. Mishra, S. Sadasivan, Experimental peak/total ratios for a few NaI(Tl) crystal sizes, Nucl. Instrum. Methods 69 (2) (1969) 330–334.

[14] A. Cesana, M. Terrani, Determination of the full energy peak efficiency of NaI(Tl) detectors, Int. J. Appl. Radiat. Isot. 29 (7) (1978) 427–429.